

# PRECONCEPTUAL DESIGN OF AN INJECTOR FOR AN NLC ENGINEERING TEST FACILITY<sup>†</sup>

A. M. M. Todd, H. P. Bluem, Advanced Energy Systems, P.O. Box 7455, Princeton, NJ 08543, USA  
C. L. Bohn, Fermi National Accelerator Laboratory, Batavia, IL 60510, USA

## Abstract

The preconceptual design of an S-band photo-injector system for a Next Linear Collider (NLC) Engineering Test Facility (ETF) at Fermi National Accelerator Laboratory (FNAL) has been completed. A photo-cathode gun will deliver a range of bunch charges up to 4 nC at around 190 MeV. The projected performance is  $2.5 \pi$  mm-mrad rms normalized transverse emittance at 1 nC and  $6.7 \pi$  mm-mrad at 3.6 nC bunch charge, for 0.5 mm rms radius spherical bunches with an energy spread of less than 0.1%. We describe the proposed beamline and the performance achieved in end-to-end simulations.

## 1 INTRODUCTION

The design of an injector for an NLC [1] ETF [2] at FNAL has been performed. This design was undertaken to develop the achievable performance that could be expected and to determine a rough order of magnitude cost estimate for the facility. The performance and cost parameters achieved suggest that the proposed S-band facility is viable.

The target performance specifications are summarized in Table 1 together with the corresponding performance actually achieved in end-to-end simulations for three specific bunch charge levels. The simulation results quoted utilized 10,000 particles and we have performed studies that verify that these results are converged to within ~5%. We describe the various components that comprise the injector and their function in achieving these specifications. We also summarize the physics design and illustrate the performance with three bunch charge levels that span the proposed operating range.

## 2 BEAMLINE DEFINITION & ANALYSIS

The injector system consists of three sections with specific performance roles. Fig. 1 shows the longitudinal and transverse beam envelopes along the system for a 1.0 nC bunch charge case with these various sections identified. This figure, which is the output of a TOPKARK code [3] simulation, does not include the gun itself and the bulk of the solenoid field, which are to the left of the figure and separately simulated in the MRC MAGIC code [4].

The first section of the injector consists of a photo-cathode gun and solenoid, a drift space and then a standard SLAC S-Band traveling-wave accelerating structure. The accelerating gradient in all four of the SLAC S-Band structures is restricted to 20 MV/m. The gun and solenoid are patterned after the Brookhaven Gun IV design [5]. The solenoid strength, drift space and accelerator gradient are chosen to optimize the transverse emittance compensation [6] of the system in order to deliver the brightest possible beam. In addition, the accelerator strength and phase must also be adjusted to perform the longitudinal phase space manipulation of the second section of the injector. This then influences the emittance compensation settings and requires some iteration.

As illustrated by the transverse beam and emittance envelopes of Figs. 1 and 2, the emittance compensation prescription calls for setting the solenoid to deliver a near-waisted beam at the entrance of the first accelerating structure. The required gradient in the accelerator is related to the input beam size and should focus the beam down to again deliver a near-waisted beam at the accelerator exit.

Table 1: Target ETF Injector Performance Compared to Values Achieved in End-to-End Simulations

Parameter	Units	Target	1 nC	2 nC	4 nC
Bunch Charge	nC	1 - 4	0.98	1.88	3.62
Output Energy	MeV	> 100	193	185	193
X Normalized RMS Emittance	$\pi$ mm- mrad	< 10	2.42	5.30	6.81
Y Normalized RMS Emittance	$\pi$ mm- mrad	< 10	2.48	4.98	6.57
X Beam RMS Spot	mm	< 0.5	0.12	0.46	0.44
Y Beam RMS Spot	mm	< 0.5	0.16	0.41	0.50
Z Bunch RMS Half-Length	mm	< 0.5	0.48	0.50	0.62
Energy Spread ( $\Delta W / W$ )	%	< 0.2	0.08	0.18	0.09
Bunch Train "Macropulse" @ 2.8 nsec Pulse Spacing		1 - 95	1 - 95	1 - 95	1 - 95
Projected CSR Emittance Growth in Chicane	%	< 10	~ 5	~ 6	~ 9

<sup>†</sup> Work supported by Universities Research Association, Inc., under U.S. DoE Contract DE-AC02-76CH00300 through Fermi National Accelerator Laboratory Purchase Order 532383.

## BEAM ENVELOPES

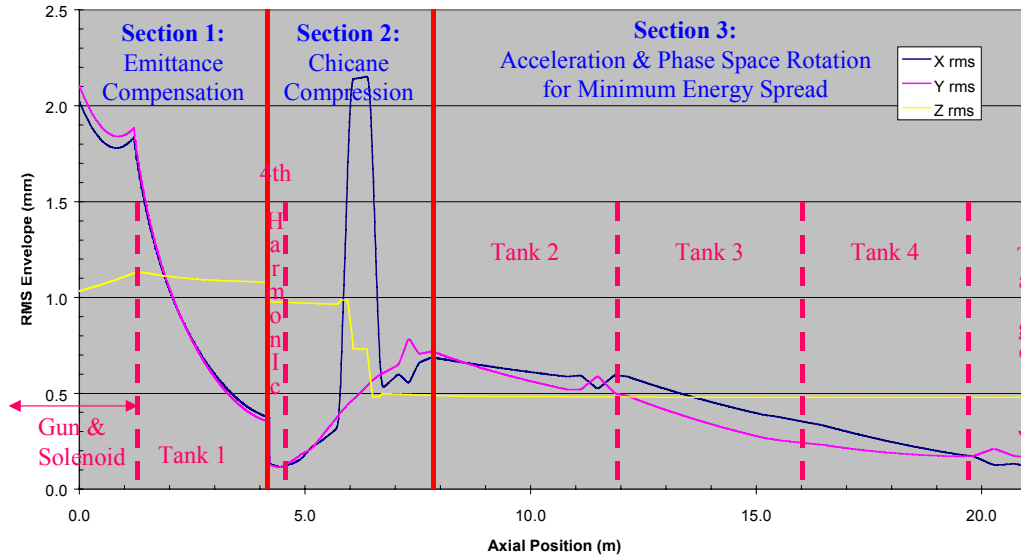


Figure 1: 1 nC Beam Envelopes Along the Injector with Functional Beamline Components Identified

The second section of the injector performs beam clean-up and manipulates the longitudinal phase space to achieve the short pulse and energy spread requirements. The phase and energy of the first accelerating structure are set to orient the beam for compression in a chicane to achieve the desired bunch length of less than 0.5 mm. As noted, the resultant acceleration in the accelerator structure has also to satisfy the emittance compensation specifications. The dispersion in the chicane and the focusing from the triplets before and after it can be seen in Fig. 1. The beam is permitted to expand a little through this section to set up the acceleration and focusing in the third section of the beamline.

The parameters of the chicane were chosen to control coherent synchrotron radiation (CSR) emittance growth effects. Following Ref [7], we chose to minimize the bend length and angle required to achieve the desired compression. We estimate that the resultant emittance growth due to CSR, which is not modeled in our simulations, will be restricted to less than 10%. This will not compromise the delivery of the specified target beam performance.

Our initial modeling of the system resulted in longitudinal phase space curvature that could not be rotated later to achieve the required energy spread. The curvature from front to back of the bunch, which is initially created in the photocathode gun and amplified in the chicane, created an eyebrow-shaped phase space at the end of the injector. We initially tried to cure this curvature by adjusting the focussing in the chicane. In principle, using combined function dipoles with a field index should permit straightening of the longitudinal phase space. However, the chicane performance is very sensitive to the dipole focusing used, and this approach is self-defeating.

Instead, we inserted a twenty cell, fourth harmonic 11.424 GHz NLC structure right after the first S-Band linac. The accelerating gradient in this cavity was restricted to 50 MV/m. We are able to impress the small amount of inverse curvature on the longitudinal phase space that yielded the desired near-linear longitudinal phase space beam after the chicane.

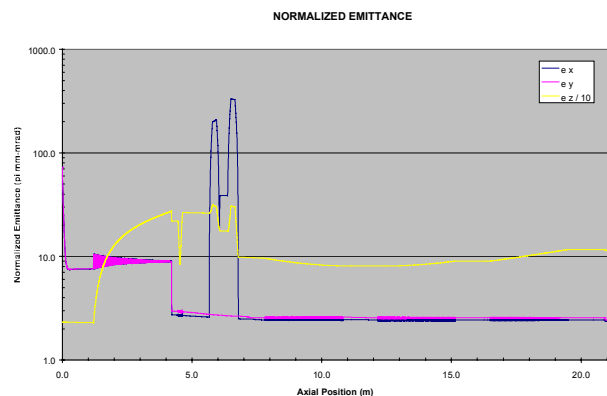


Figure 2: 1 nC Normalized RMS Emittance Envelopes

The other function of this segment is beam clean-up which is performed by scraping  $\sim 10\%$  of the beam in each case at the exit of the first linac. The beam removed is from the aberrated front of the bunch that can be seen in the Fig. 3 phase space plots of the beam delivered by the photocathode gun. We find that the aberrated longitudinal particles are correlated with the outlying particles of the transverse-phase-space plots. At the beam clean-up location, where the phase space is more-or-less upright, these particles tend to appear as a jet at 90 degrees to the main transverse phase space, which is why this location was selected for the scrapers. The impact of this clean-up

can be seen as an effective reduction of the envelope size at the scraper point in the envelope plots of Fig. 1 and the emittance of Fig. 2.

The final section of the injector is the accelerating section. We use three SLAC structures identically phased to accelerate the beam to between 150 and 200 MeV, while simultaneously rotating the phase space for minimum energy spread. The longitudinal bunch length is locked in after the chicane. Various combinations of the gradient and phasing in these structures can be used to achieve different output energy with minimum energy spread. If only two tanks are used, the achievable energy spread for the high-charge case rises to about 0.25% but the cost of the overall system is obviously reduced. A focusing triplet is included between each accelerating structure and at the end of the system. The magnets are used, as illustrated by Fig. 1, to symmetrize the transverse beams along the system and to properly arrange for near-waisted, circular input to each accelerating structure.

Table 1 summarized the performance achieved for three different bunch charge levels, namely, 1, 2 and 4 nC. The MAGIC output from the gun modeling is passed directly to the high-order space-charge code, TOPKARK, for modeling the remainder of the beam line in these end-to-end simulations. Fig. 2 shows that the transverse emittance is controlled throughout the beamline after the beam leaves the emittance-compensation-solenoid fringe field and the longitudinal emittance drops when the beam has been straightened out after the chicane. The transverse emittance invariant plotted includes the vector potential of the solenoid field that accounts for the drop in emittance as the beam emerges from that fringe field in the emittance compensation section.

Finally, we show in Figs. 4 and 5, phase space puncture plots for the 1 and 4 nC cases respectively after passage through the three accelerating linacs and the final focussing triplet. The rotation of the longitudinal phase space for minimum energy spread is evident.

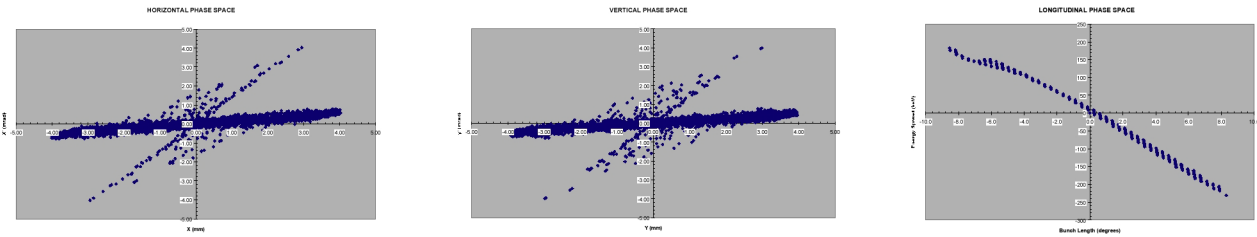


Figure 3: 1 nC Phase Space Plots (X, Y, Z) After the Photo-Cathode Gun

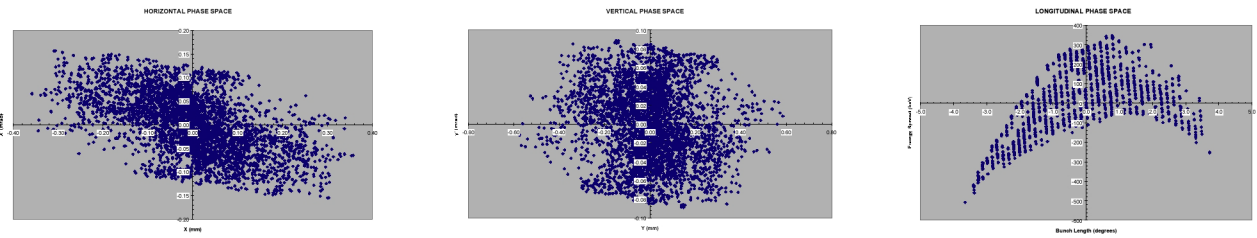


Figure 4: 1 nC Phase Space Plots (X, Y, Z) at the Injector Output

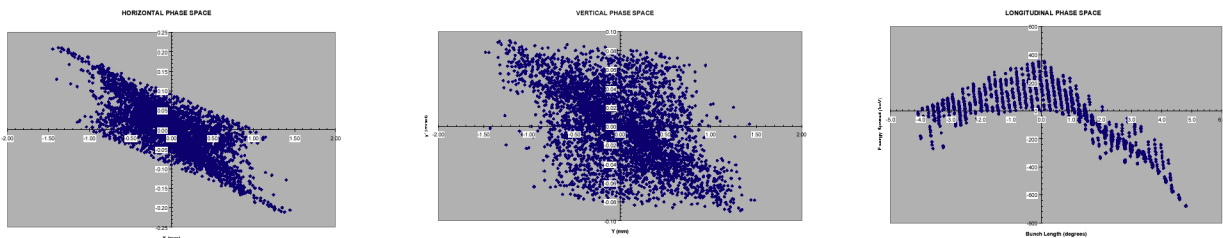


Figure 5: 4 nC Phase Space Plots (X, Y, Z) at the Injector Output

### 3 CONCLUSIONS

The use of an S-Band injector for an NLC ETF appears feasible. A physics design has been completed that delivers the required system performance over the operating range prescribed. The resultant injector system cost appears to be within the budgetary range.

### 4 REFERENCES

- [1] [http://www-project.slac.stanford.edu/lc/ZDR/nlc\\_zeroth.htm](http://www-project.slac.stanford.edu/lc/ZDR/nlc_zeroth.htm)
- [2] C. L. Bohn et al., these Proceedings.
- [3] D.L. Bruhwiler et al., AIP Conf. Proc. **297** 524 (1993).
- [4] B. Goplen et al., *Comp. Phys. Comm.* **87**, 54 (1995).
- [5] D.T. Palmer et al., Proc. PAC97, 2687 (1998).
- [6] B. E. Carlsten, Proc. PAC89, 313 (1989).
- [7] <http://www.slac.stanford.edu/pubs/slacreports/slac-r-521.html>